
Nov 6th, 12:00 AM - 12:00 AM

Effect of Stressed-Skin Action on Optimal Design of a Cold- Formed Steel Portal Framing System

Duoc T. Phan

Andrzej M. Wrzesien

James B. P. Lim

Iman Hajirasouliha

Follow this and additional works at: <https://scholarsmine.mst.edu/isccss>



Part of the [Structural Engineering Commons](#)

Recommended Citation

Phan, Duoc T.; Wrzesien, Andrzej M.; Lim, James B. P.; and Hajirasouliha, Iman, "Effect of Stressed-Skin Action on Optimal Design of a Cold-Formed Steel Portal Framing System" (2014). *International Specialty Conference on Cold-Formed Steel Structures*. 4.

<https://scholarsmine.mst.edu/isccss/22iccfss/session09/4>

This Article - Conference proceedings is brought to you for free and open access by Scholars' Mine. It has been accepted for inclusion in International Specialty Conference on Cold-Formed Steel Structures by an authorized administrator of Scholars' Mine. This work is protected by U. S. Copyright Law. Unauthorized use including reproduction for redistribution requires the permission of the copyright holder. For more information, please contact scholarsmine@mst.edu.

EFFECT OF STRESSED-SKIN ACTION ON OPTIMAL DESIGN OF A COLD-FORMED STEEL PORTAL FRAMING SYSTEM

Duoc T. Phan¹, Andrzej M. Wrzesien², James B.P. Lim³, Iman Hajirasouliha⁴

Abstract

Cold-formed steel portal frames can be a viable alternative to conventional hot-rolled steel portal frames. They are commonly used for low-rise commercial, light industrial and agricultural buildings. In this paper, the effect of semi-rigid joints and stressed-skin action are taken into account in the optimal design of cold-formed steel portal frames. A frame idealization is presented, the results of which are verified against full-scale. A real-coded niching genetic algorithm (RC-NGA) is then applied to search for the minimum cost for a building of span of 6 m, height-to-eaves of 3 m and length of 9 m, with a frame spacing of 3 m. It was shown that if stressed-skin action and joints effects are taken into account, that the wind load cases are no longer critical and that the serviceability limit state controls for the gravity load case with the apex deflection binding. It was also shown that frame costs are reduced by approximately 65%, when compared against a design that does not consider stressed-skin action, and 50% when compared against a design based on rigid joints.

Keywords: cold-formed steel, stressed-skin action, optimization

¹ Assistant Professor, Department of Civil Engineering, Faculty of Engineering and Science, Universiti Tunku Abdul Rahman, Kuala Lumpur, Malaysia

² PhD student, Department of Civil Engineering, University of Strathclyde, Glasgow, UK

³ Senior Lecturer, Department of Civil Engineering, University of Auckland, Auckland, New Zealand

⁴ Lecturer, Department of Civil & Structural Engineering, The University of Sheffield, Sheffield, UK

1. Introduction

Cold-formed steel portal frames (see Fig. 1) can be a viable alternative to conventional hot-rolled steel portal frames. As can be seen from Fig. 1, cold-formed steel channel-sections are used for the purlins and side rails, as well as for the columns and rafter members. Sheeting is fastened directly to the flanges of columns and rafter members. The joints are formed through brackets bolted to the cold-formed steel channel-sections, typically using an array of 3x3 bolts for each bolt-group, as shown in Fig. 2.



Figure 1: Photograph of a cold-formed steel portal framing system

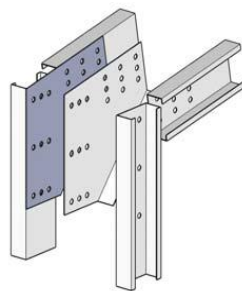


Figure 2: Details of eaves joint

Such cold-formed steel portal frames are commonly used for low-rise commercial, light industrial and agricultural buildings. However, while spans of up to 20 m are achievable (Lim and Nethercot 2004), the majority of such buildings constructed are small, only having spans of around 6 m and lengths of around same order. The resulting “box-shaped” buildings when clad can behave differently from conventional bare frames due to the stiffening effect of roof diaphragms (Davies and Bryan 1982). This phenomenon, referred to as stressed-skin action (see Fig. 3), is particularly important for small buildings.

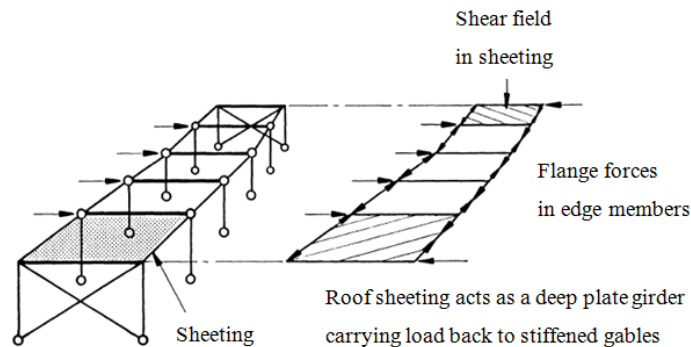


Figure 3: Stressed-skin action under horizontal load buildings (after BS 5950-Part 9)

A related paper by Wrzesien *et al.* (2014) has been concerned with experimentally determining the effect of stressed-skin action for such small cold-formed steel buildings. Buildings of span of 6 m, height-to-eaves of 3 m and length of 9 m were tested, having a frame spacing of 3 m. The experimental tests included quantifying the rotational stiffness of the joints and cladding.

In this paper, a design optimization of buildings having the same geometry as the ones tested by Wrzesien *et al.* (2014) is presented. The design optimization uses a real-coded niching genetic algorithm (RC-NGA). The results of the design optimization are used to quantify the beneficial effects of stressed-skin action in design. The semi-rigidity and partial strength of the joints are taken into account as part of the design process. The frames are designed in accordance with the British Standards for cold-formed steel, to both ultimate

and serviceability limit states. All wind load combinations are taken into account in accordance with BS 6399 (2002).

2. Frame loading

The design loads to be applied to the building as part of the design optimization are as follows:

Dead load (DL): 0.15 kN/m^2 (including cladding and service) and self-weight of members of columns, rafters, purlins, and side rails

Live load (LL): 0.6 kN/m^2

It is assumed that the dynamic wind pressure (q_s) is 1.0 kN/m^2 . In accordance with BS6399 (2002), the design wind pressures acting on each of the four sides of the frame are obtained by multiplying q_s by a coefficient of pressure and other related factors. The coefficient of pressure acting on each face is obtained from a combination of the external pressure coefficient C_{pe} and the internal pressure coefficient C_{pi} . The eight wind load combinations acting on the frame and their corresponding coefficients for both side wind and end wind, as provided in BS6399, are considered.

The frame design is checked at the ultimate limit state for the following ultimate load combinations (ULCs):

$$\text{ULC1} = 1.4\text{DL} + 1.6\text{LL} \quad (1a)$$

$$\text{ULC2} = 1.2\text{DL} + 1.2\text{LL} + 1.2\text{WL} \quad (1b)$$

$$\text{ULC3} = 1.4\text{DL} + 1.4\text{WL} \quad (1c)$$

$$\text{ULC4} = 1.0\text{DL} + 1.4\text{WL} \text{ (for wind uplift)} \quad (1d)$$

The frame is also checked at the serviceability limit state, using deflection limits recommended by the Steel Construction Institute (SCI) (see Table 1), for the following serviceability load combinations (SLCs):

$$\text{SLC1} = 1.0\text{LL} \quad (2a)$$

$$\text{SLC2} = 1.0\text{WLC} \quad (2b)$$

Table 1. Deflection limits for steel portal frames after SCI

Test	Absolute deflection	Differential deflection relative to adjacent frame
Lateral deflection at eaves	$\leq \frac{h_f}{100}$	$\leq \frac{b_f}{200}$
Vertical deflection at apex	-	$\leq \frac{b_f}{100}$ and $\sqrt{b_f^2 + s_f^2}/125$

where h_f is column height; b_f is frame spacing; and s_f is rafter length.

3. Frame design

The frame is analyzed using first-order analysis. The frame analysis is embedded in the optimal algorithm to analyze each candidate solution in each generation for optimization process (Phan *et al.* 2013). For each ultimate load combination, the bending moment, shear force and axial force diagrams for the frame are determined. These results are then passed to design modules to carry out the member checks at the critical sections or segments between two lateral restraints. In this paper, the effective width method (EWM) was applied to work out the section capacities in axial, shear, and bending.

For frame design, the columns and rafters are checked for combined axial force (either tension or compression) and bending moment as well as combined shear and bending, according to BS5950-5 (1998). The normalized forms of the design constraints given in BS5950-5 are expressed as follows:

The combined tension and bending moment check is:

$$g_1 = \frac{F_t}{P_t} + \frac{M_x}{M_{cx}} \leq 1 \quad (3)$$

where

- F_t is the applied tensile load at the critical section
- P_t is the tensile capacity of a member, which is calculated from effective net area A_e of the section and design strength p_y of 390 N/mm²
- M_x is the applied bending moment at the critical section

M_{cx} is the moment capacity in bending about x axis.

For the semi-rigid joints, the moment capacity of members in the vicinity of the joint is reduced as described by Lim and Nethercot (2003)

The combined compression and bending moment is checked for local capacity at positions having greatest bending moment and axial compression and for lateral torsional buckling:

For the local capacity check:

$$g_2 = \frac{F_c}{P_{cs}} + \frac{M_x}{M_{cx}} \leq 1 \quad (4)$$

where

F_c is the applied compression load at the critical section

P_{cs} is the short strut capacity subjected to compression, which is calculated from effective net area A_e of the section and design strength p_y of 390 N/mm².

For the lateral torsional buckling check:

$$g_3 = \frac{F_c}{P_c} + \frac{M_x}{M_b} \leq 1 \quad (5)$$

where

P_c is the axial buckling resistance in the absence of moments

M_b is the lateral resistance moment about major axis.

For members subjected to both shear and bending moment, the webs of members should be designed to satisfy the following relationship:

$$g_4 = \left(\frac{F_v}{P_v} \right)^2 + \left(\frac{M_x}{M_{cx}} \right)^2 \leq 1 \quad (6)$$

where

F_v is the shear force in associate with the bending moment M_x at the same section

P_v is the shear capacity or shear buckling resistance

In accordance with BS 5950-Part 9 (1998), the roof diaphragm is assumed to transfer the horizontal load to stiff gables, thus reducing the level of loading applied to the internal frames. This allows lightening of the internal frames. When the ultimate shear capacity of the roof diaphragm is reached, the load is no longer redistributed and the internal frames are subjected to a larger load. The following check must therefore be satisfied if stressed-skin design is to be used safely:

$$g_{5a} = \frac{V_{d,u}}{V_d} \leq 1 \quad (7a)$$

$$g_{5b} = \frac{V_{d,s}}{0.6V_d} \leq 1 \quad (7b)$$

where:

$V_{d,u}$ is the applied shear force at the ultimate limit state loading along the diaphragm expressed as a diagonal force

$V_{d,s}$ is the applied shear force along the diaphragm expressed as a diagonal force under serviceability load

V_d is the design shear capacity of the diaphragm expressed as a diagonal force obtained from experiment

For serviceability limit state checks, the deflections at eaves and apex should be satisfied the following constraints:

$$g_6 = \frac{\delta_e}{\delta_e^u} \leq 1 \quad (8a)$$

$$g_7 = \frac{\delta_a}{\delta_a^u} \leq 1 \quad (8b)$$

where:

δ_e is the horizontal deflection at eaves under the action of serviceability load

δ_a is the vertical deflection at apex under the action of serviceability load

δ_a^u and δ_e^u are the maximum permissible vertical and horizontal deflections, respectively as shown in Table 1

5. Optimization formulation

The objectives of the design optimization are to satisfy the design requirements and minimize the cost of the channel-sections and brackets for the internal frame per unit floor area. The material cost depends on the frame spacing, frame geometry, cross-section sizes of structural members, and sizes of eaves and apex bracket, which can be expressed as:

$$C = \frac{1}{L_f b_f} \left[\sum_{i=1}^m c_i l_i + w_{br} c_{br} \right] \quad (9)$$

where:

- C is the cost of the building per square meter of floor area
- c_i are the costs per unit length of cold-formed steel sections for frame members and secondary members
- l_i are the lengths of cold-formed steel frame members
- m is the number of structural members in the portal frame
- c_{br} is the cost per unit weight of the brackets
- w_{br} is the total weight of the brackets

The objective function contains five decision variables consisting of the size of the columns and rafters (discrete variable) being selected from a list of sections available in the UK (see Table 3), and the length of bolt-groups (continuous variables), used at the eaves and apex joint, which varies within the range 100 mm to 2000 mm. It should be noted that the width of the bolt-groups depends on the depth of the members. The optimum solution for such design variables, which produces the lowest cost for the objective function, is searched in the design space subjected to the relevant design constraints as described in Section 3.

Table 2. Properties of cold-formed steel channel sections

Section	D (mm)	B (mm)	t (mm)	M_c (kNm)	k_b (kN/mm)	Weight (kg/m)	Cost (£/m)
C15014	152	64	1.4	6.49	4.72	3.29	4.04
C15016	152	64	1.6	7.91	5.27	3.76	4.23
C15018	152	64	1.8	9.24	5.81	4.21	4.74
C15020	152	64	2.0	10.48	6.32	4.67	5.19
C20015	203	76	1.5	10.29	5.00	4.38	5.02
C20016	203	76	1.6	11.44	5.27	4.67	5.31
C20018	203	76	1.8	13.74	5.81	5.25	5.98
C20020	203	76	2.0	15.93	6.32	5.82	6.56
C20025	203	76	2.5	20.96	7.50	7.23	8.12
C25018	254	76	1.8	17.36	5.81	5.96	7.00
C25020	254	76	2.0	20.26	6.32	6.61	7.95
C25025	254	76	2.5	27.03	7.50	8.21	9.88
C25030	254	76	3.0	33.35	8.57	9.79	11.82
C30025	300	95	2.5	36.42	7.50	9.80	11.18
C30030	300	95	3.0	46.01	8.57	11.69	13.04

6. Comparison against experimental results

Table 3 summaries the six frame tests of Wrzesien *et al.* (2014) that are used to validate the analytical model.

Table 3. Summary of full-scale frame tests after Wrzesien *et al.* (2014)

Test	Bolt-group size	Load direction	Sheeting
A1	160 mm x 80 mm	Vertical	No
A2		Horizontal	Yes
A3			
B1	280 mm x 80 mm	Vertical	No
B2		Horizontal	Yes
B3			

Figure 4 shows the variation of vertical load against apex deflection for the frame tests. For Test A1, there is a large initial vertical deflection of 80 mm, which can be attributed to bolt-hole misalignment. The results of a frame analysis are also shown; as can be seen, the results are offset along the deflection axis to enable a comparison to be made at loads when all the bolt-holes are in full bearing against the bolt-shanks. There is good agreement between the tests and analytical results.

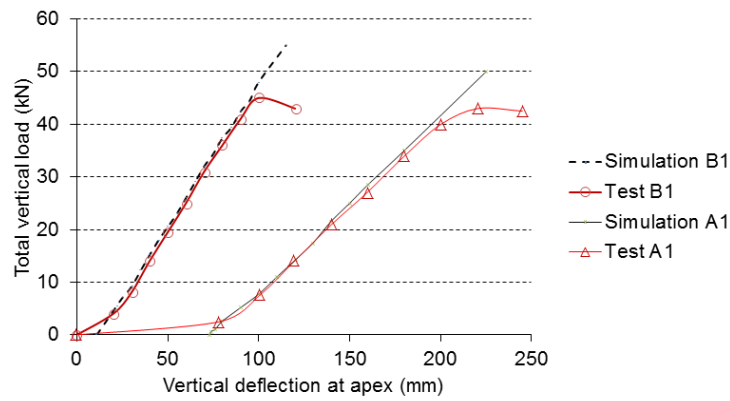
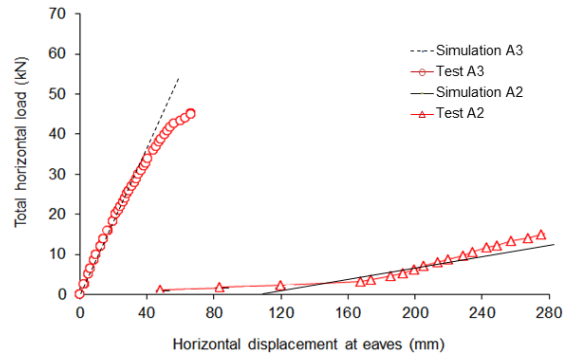
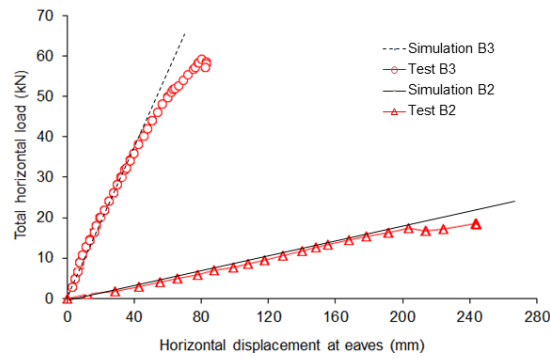


Figure 4: Variation of vertical load against apex deflection

The stiffness and strength of the cladding were experimentally determined to be 3.49 kN/mm and 38.24 kN, respectively. Figure 5 shows the variation of horizontal load against deflection at the eaves. As can be seen, there is also good correlation between the experimental and analytical results.



(a) Tests A2 and A3



(a) Tests B2 and B3

Figure 5: Variation of horizontal load against apex deflection

7. Real-coded niching genetic algorithm (RC-NGA)

In the proposed RC-NGA, tournament selection using niching is applied. The process is conducted by selecting two random individuals from the current population. The normalized Euclidean distance between two solutions is computed. If this Euclidean distance is smaller than an empirical user-defined critical distance, these solutions are compared using their fitness function values. Otherwise, they are not compared and another solution is selected at random from the population for comparison. If after a certain number of checks, no solution is found to satisfy the critical distance, the first one is selected for

the crossover operation. In this way, only solutions in same region (or niche) compete against each other for selection and crossover. Moreover, the convenience of using RC-GA is that genetic operators, namely simulated binary crossover (SBX) and polynomial mutation, are directly applied to the design variables without coding and decoding as compared with the binary string GAs (Deb 2001).

A penalty function is used to transform this constrained problem to an unconstrained one. Penalty values are imposed empirically, in proportion to the severity of constraint violation based on the ultimate limit state design. The fitness function adopted has the form:

$$F = C(1 + \sum_{i=1}^n CVP_i) \quad (11)$$

where

F is the fitness function

CVP_i is the constraint violation penalty for the i th constraint

n is the number of design constraints

The proposed optimization procedure aims to minimize the value of the fitness function F (Eq. 11). This is achieved by minimizing the cost C and reducing the penalty CVP_i to zero. The procedure involves RC-NGA and frame analysis modules (Phan *et al.* 2013). In this optimization process, the evaluation process computes the fitness function values using the objective function (Eq. 10) along with the corresponding penalty values. Better solutions will yield smaller fitness values, and consequently are selected preferentially by the tournament selection operator. The criterion for terminating the program is a predefined total number of generations.

8. Optimum result and discussion

The design optimization will consider the same building geometry tested by Wrzesien *et al.* (2014). The GA parameters used are as follows: population size = 80; crossover probability $p_c = 0.9$; mutation probability $p_m = 0.1$; niching

radius = 0.25; termination criterion = 200 generations; distribution coefficient for mutation = 1.0; distribution coefficient for crossover = 1.0. The maximum number of function evaluations allowed was 16000. The initial populations were generated randomly. The results obtained from an optimization process showed that the standard deviations of the best cost achieved are consistently small, and diversity among the population of solutions is maintained in all the generations in the optimization. This provides assurance that the convergence achieved was not spurious.

Using RC-NGA, the cold-formed steel portal framing system was optimized for the following three Design Assumptions (DAs):

DA1: Rigid joints and no stressed-skin action

DA2: Semi-rigid joints and no stressed-skin action

DA3: Semi-rigid joints and stressed-skin action

Each of the three Design Assumptions leads to an optimal design specification for the sections and bolt-group sizes. Table 4 shows the sections and bolt-group sizes for each specification. S1 is the optimal design obtained from DA1. Similarly, S2 and S3 are the optimal design specifications obtained from DA2 and DA3, respectively. Table 5 shows the frame and joint costs for each specification. As can be seen, the column and rafter sizes for S3 are lower than those of either S1 or S2. For the case of S1, only the cost of the sections is included.

Table 4. Cross-section and bolt-group sizes for each specification

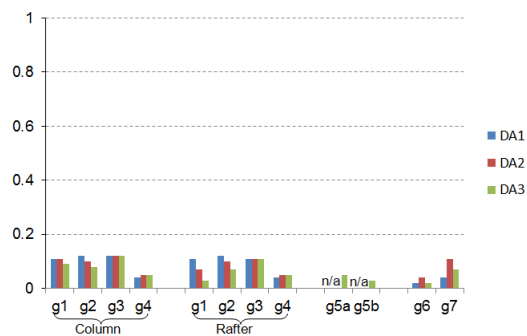
	Cross-section		Bolt-group size		
	Column	Rafter	Eaves rafter	Eaves column	Apex
			$a_{er} \times b_{er}$ (mm×mm)	$a_{ec} \times b_{ec}$ (mm×mm)	$a_{ar} \times b_{ar}$ (mm×mm)
S1	BBC25020	BBC25020	-	-	-
S2	BBC30025	BBC30025	470x210	470x210	350x210
S3	BBC15014	BBC15014	150x80	150x80	150x80

Table 6. Frame and joint costs for each specification

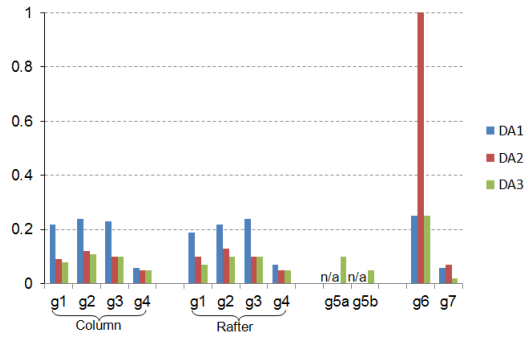
	Frame cost (£/m ²)	Joint cost (£/m ²)	Total (£/m ²)
S1	10.68	-	-
S2	15.06	5.27	20.33
S3	5.44	1.38	6.82

Figure 6 show the unity factors of S2 under each of the three DAs. The unity factors are separated into the gravity load case (ULC1) and the critical wind load case, which was shown to be ULC2. It can be seen that the design is controlled by SLS, with the horizontal deflection of the eaves under ULC2 being critical.

Figure 7 shows the unity factors of S3, again under each of the three DAs. As can be seen, the design is also controlled by SLS, but this time the apex deflection under the gravity load case is critical. It can be noted that the value of q_s would need to more than double in order for the wind load case to be critical. It can also be seen that the column and rafter sections could be sized on the basis of rigid joints, under only a ULS for the gravity load case (i.e. for this building, if stressed-skin action is not taken into account, the wind load cases can be ignored and the column and rafter sections sized on a rigid joint assumption).

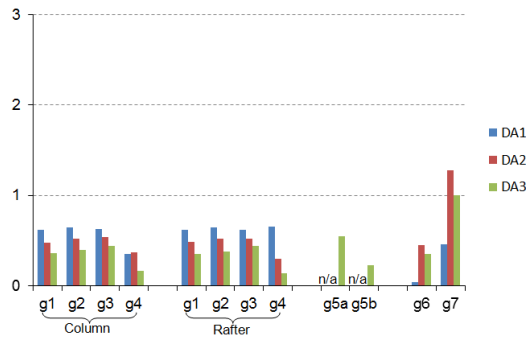


(a) Gravity load combination (ULC1)

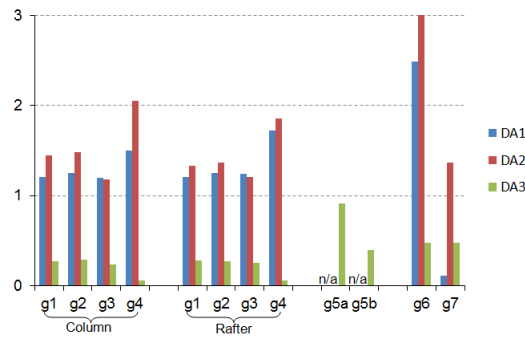


(b) Critical wind load combination (ULC2)

Figure 6: Unity factors for S2 under each DA



(a) Gravity load case (ULC1)



(b) Critical wind load combination (ULC2)

Figure 7: Unity factors of S3 under each DA

9. Conclusions

A real-coded genetic algorithm has been used to determine the optimal design of a cold-formed steel portal frame. The building considered was of span of 6 m, height-to-eaves of 3 m and length of 9 m, with a frame spacing of 3 m. It was shown that if stressed-skin action and joints effects are both taken into account, that the wind load cases are no longer critical and that the serviceability limit state controls with the apex deflection binding. It should be noted that stressed-skin action has little effect on the apex deflection. It was also shown that if the column and rafter members are sized on the basis of rigid joints using only the ultimate limit state for the gravity load case, that the resulting section sizes will be still be conservative.

Appendix. – References

- British Standards, 1994. *BS5950: Structural use of steelworks in building. Part 9, Code of practice for stressed skin design*. London: British Standards Institution.
- British Standards, 2002. *BS6399: Loading for buildings*. London: British Standards Institution.
- Davies J.M., Bryan E.R., 1982. *Manual of stressed skin diaphragm design*. London: Granada.
- Deb, K., 2001. *Multi-objective optimization using evolutionary algorithms*. Chichester: John Wiley and Sons, Inc.
- Lim, J.B.P., Nethercot, D.A., 2003. Ultimate strength of bolted moment-connections between cold-formed steel members. *Thin-Walled Structures*, 41, 1019-1039.
- Lim, J.B.P., Nethercot, D.A., 2004. Finite element idealization of a cold-formed steel portal frame. *Journal of Structural Engineering, ASCE*, 130(1), 78-94, 2004.

- Phan, D.T., Lim, J.B.P., Sha, W., Siew, C.Y.M., Tanyimboh, T.T., Issa, H.K.,
Mohammad, F.A., 2013. Design optimization of cold-formed steel portal frames
taking into account the effect of topography. *Engineering Optimization*, 45:415–
33.
- Wrzesien, A.M., Lim, J.B.P., Lawson, R.M., 2014. Effect of stressed-skin action on the
behavior of cold-formed steel portal frames. Submitted to 22nd International
Specialty Conference on Cold-Formed Steel Structures.